

NOTE AND CORRESPONDENCE

Wavelet Transform and 3-Component Seismogram Analysis

Chiou-Fen Shieh¹ and Jim Wang¹

(Manuscript received 15 July 1996, in final form 30 December 1996)

ABSTRACT

A mathematical tool, namely “wavelet transform” which can capture the local structure of the signals in the time-frequency domain, is introduced for its novel application to 3-component seismogram analysis. A link between wavelet transform and polarization analysis is tested in this article. The parameters of polarization analysis in the time-frequency domain include the phase difference, the strike and the strength of polarization, and ellipticity. Through the wavelet transform, the characteristics of the above parameters are time and frequency dependent (unlike traditional analysis) and allows analysis of signals not only with respect to time, but also to different frequency components. This can provide very interesting and useful information. A 3-component synthetic seismogram is used to explain its potential application.

(Key words: Wavelet transform, Time-frequency, Polarization)

1. INTRODUCTION

While Fourier analysis and its variations are very useful mathematical tools, practical applications require basis modifications. These modification aim at “localizing” the analysis, so that it is not necessary to have the signal over $(-\infty, \infty)$ to perform the transform (as required with the Fourier integral) and so that local effects can be captured with some accuracy. The classic example is the short-time Fourier, or Gabor transform (Allen and Rabiner, 1977).

In recent years, there has been a renewed interest in the development of time-frequency representations (TFR) and in gaining a better understanding of the concept of the time-varying signals. In many situations involving nonstationary signals, it is advantageous to display a signal over a joint time-frequency plane using a TFR. TFR provide a measure of the time-varying spectral content of a signal. Some of the earlier TFR used include the spectrum, the Wigner distribution, the Rihaczek distribution, and the Page distribution (Cohen, 1989). A number of review papers and numerous research paper have been published on this topic in the past few years.

¹Institute of Seismology and Applied Geophysics, National Chung Cheng University, Chia-Yi, Taiwan, ROC

Linear transforms for time-frequency analysis were first proposed by Gabor (1946). Gabor suggested that a time-frequency description of a signal could be obtained by performing Fourier analysis on the signal as it appear when seen through a set of identical windows that are translated with respect to each other in time. Gabor suggested the use of Gaussian windows, because they are simultaneously well localized in the time and frequency domains. Gabor's method has been extended to a set of methods known collectively as short-time Fourier transform (Allen and Rabiner, 1977). The different methods in this body of work employ different shaped windows.

Both the Gabor transform and the short-time Fourier transform have the property whereby the bandwidth of the analyzing function is a constant independent of central frequency; likewise the time duration of the analyzing function is constant. In some application it is felt that the analyzing functions should have a constant bandwidth-to-center-frequency ratio. The wavelet transform, which was first introduced in 1986 by Lemarié and Meyer and which has received considerable attention in the mathematical and engineering communities, does indeed have this property. The name "wavelet" had been used previously in the literature, but its current meaning is due to Goupillaud *et al.* (1984), and Grossman and Morlet (1984). The simplicity and elegance of the wavelet method was appealing and mathematicians started studying wavelet analysis as an alternative to Fourier analysis. This led to the discovery of wavelets which form orthonormal bases for square-integrable and other function spaces by Meyer (1990), Daubechies (1988) and others. A formalization of such constructions by Mallat (1989) and Meyer (1990) created a framework for wavelet expansions called multiresolution analysis, and established links with methods used in other fields. In fact, may be one of the biggest contributions of wavelets has been to bring people from different fields together, resulting in a cross fertilization and exchange of idea and methods that has led to progress in various fields. Yet although wavelet theory is rather new, it may be noted at the outset that many of the idea underlying wavelets are not new. Indeed, wavelet theory can be viewed as a convenient and useful mathematical framework for formalizing and relating some well-established methodologies from a number of diverse areas. The abundance of useful features illustrated by wavelets and wavelet transform has led to their application to a wide range of signal processing problems. Although the vital relationship between wavelet theory and idea from signal processing are well known, the application of wavelet theory to the study of seismograms is not well discussed. This article aims to bridge this gap with the feature of wavelet-based seismograms analysis. A set of synthetic 3-component data are analyzed to explain its potential application in the near future.

2. WAVELET TRANSFORM

The analysis, or the basis, functions for the wavelet transform are generated from a single "mother function" by the process of shifting and scaling. The most important quality of the wavelet basis functions is that they can be made orthogonal, and yield an orthogonal decomposition for other function shapes.

Consider the family of functions obtained by shifting and scaling a "mother wavelet" $\phi(t)$,

$$\phi_{a,b}(t) = \frac{1}{\sqrt{a}} \phi\left(\frac{t-b}{a}\right) \quad (1)$$

where a and b are scale and shift parameters, respectively, and the factor $1/\sqrt{a}$ is used to conserve the norm. The mother wavelet we chose was not arbitrary, but rather it satisfied a zero-mean condition. There are many choices with different purposes and/or different algorithms in selecting different “mother wavelets” (Coifman and Wickerhauser, 1992; Daubechies, 1992; Meyer, 1993; Mallat and Zhang, 1993). In this study, the basis wavelet $\phi(t)$ in Equation (1) is chosen as a harmonic wave modulated by a Gaussian envelope (Grossmann, *et al.*, 1989)

$$\phi(t) = e^{-t^2/2\sigma^2} e^{2\pi i f_0 t} \quad (2)$$

Under such conditions, the local frequency of the analysis does indeed satisfy (Rioul and Vetterli, 1991)

$$f = af_0 \quad (3)$$

As a result, this local frequency, whose definition depends on the basis wavelet, is no longer linked to frequency modulation but is now related to time-scales.

Shifts and scales can be chosen to obtain a constant relative bandwidth analysis known as the wavelet transform. The continuous wavelet transform (CWT) of a continuous-time signal $f(t)$ is defined by the convolution integral (Grossmann and Morlet, 1984)

$$CWT_f(a,b) = \frac{1}{\sqrt{a}} \int \phi^*\left(\frac{t-b}{a}\right) f(t) dt \quad (4)$$

which measures the “similarity” between the signal and the wavelets.

The time-frequency resolution of the CWT involves a tradeoff: at high frequencies the CWT is sharper in time, while at low frequencies, it is sharper in frequency. In other words, the CWT has some localized properties, in particular sharp time localization at high frequencies (a is small), which distinguishes it from traditional Fourier transform. An algorithm for computing the CWT on a grid of samples in time and scale is adapted from Jones and Baraniuk (1991). Although there are other efficient algorithms to compute CWT (Beylkin, *et al.*, 1991; Mallat and Zhang, 1993) or available DWT code from “Numerical Recipes” (Press *et al.*, 1992), the algorithm used in this article is simple and easy for readers to reproduce. For readers’ benefit, a brief description of the computational procedure follows. In principle, the CWT can be computed by first finding the Fourier transforms of the signal, $f(t)$ and the normalized wavelet, $\phi_a(t)$. Let the number of samples of the signal and wavelet be N_s and N_w , respectively. The scale parameter is discretised to a set of rational values a_i , $i=1, \dots, N_f$; where N_f is the total number of frequency range to be analyzed. The value of each a_i is determined from Equation (3), and each scaled wavelet, $\phi_a(t)$ is computed from Equation (2). Zero-padded $f(t)$ and $\phi_a(t)$ up to the M -point, where $M \geq N_s + N_w$ and is a power of 2. The Fourier transform of $f(t)$ using M -point FFT is taken to obtain $F(f)$, and the chirp Z-transform (Rabiner and Schafer, 1969) of each $\phi_a(t)$ is taken to obtain $\Phi_a(f)$. To obtain CWT, multiply the $F(f)$ by $\Phi_a(f)$ and then take the inverse FFT.

A widely used algorithm called matching pursuit decomposes any signal into a linear expansion of wavelets that belong to a redundant dictionary of functions (Mallat and Zhang, 1993). These wavelets are selected in order to best match the signal structures. To obtain a free copy of this computer code, one can download through "ftp" at the address mentioned by Mallat and Zhang (1993) or at *MatLab* Stanford University's (Jonathan and Donoho, 1995).

3. APPLICATION

A synthetic 3-component seismogram is used to explain the TFR of wavelet transform, and is displayed in Figure 1. Figure 1-(a), 1-(b) and 1-(c) are the tangential, the radial and the vertical components, respectively. In this Figure, we are able to see the local structure of each signal in the time and frequency domain. In other words, the magnitude of the response at any specific time and frequency can be identified. This is impossible for the original signals and their Fourier spectra because they contain either time or frequency information alone. In Figure 1, the energy of high frequency body waves is very low in the range of 0~36 seconds, as displayed in the TF plots. In the time interval (36~50 second) several high mode surface waves arrive consecutively and are superimposed, such that their behaviors are complicated and difficult to analyze. However, different modes can still be identified from the separate color plots with different spectral contents as illustrated in Figure 1-(a) and 1-(c) for the Love and Raleigh waves, respectively. During the 50~64 second period in Figure 1-(a) and 1-(b), well-dispersed fundamental mode Raleigh waves appear clearly. Because of the dispersion, the TFR has a Gaussian-like shape in each component (Coifman and Wickerhauser, 1992). Such characteristics are a useful indication for detecting dispersed surface waves. As is well known, the TFR indicates that the higher mode surface waves contain more energy at a high frequency than the fundamental mode surface waves (Figure 1-(c)).

The resolution of wavelet transform is greatly affected by the wavelets chosen. Current research aims to improve the resolution by finding a method to choose the wavelet that matches best. One of the most popular example is "mpp" (Mallat and Zhang, 1993). However, "mpp" is not always able to provide the best resolution (Jonathan and Donoho, 1995). It is still a problem that has yet to be solved. A Gaussian wavelet is used in this investigation. Though It is easy to use, a Gaussian wavelet provides worse resolution in the lower frequency range. However, our purpose is to emphasize the polarization analysis of seismograms in the time-frequency domain rather than of wavelet selection.

4. WAVELET-BASED POLARIZATION ANALYSIS

Polarization analysis has been used to introduce extra parameters for the description of complex wave fields (Vidale, 1986; Shieh and Herrmann, 1990). Time domain polarization analysis is performed through the eigensolution of a constructed 3-component coherency matrix. Although a link between wavelet-based and polarization analysis was introduced by Jonathan and Park (1995), their method was applied to more sophisticated wavelet selection and polarization parameters. Recently, there is a new view of a constructed coherency matrix which allows more polarization parameters to be extracted from a complete form (Shieh, 1996). A brief description of the method is given below.

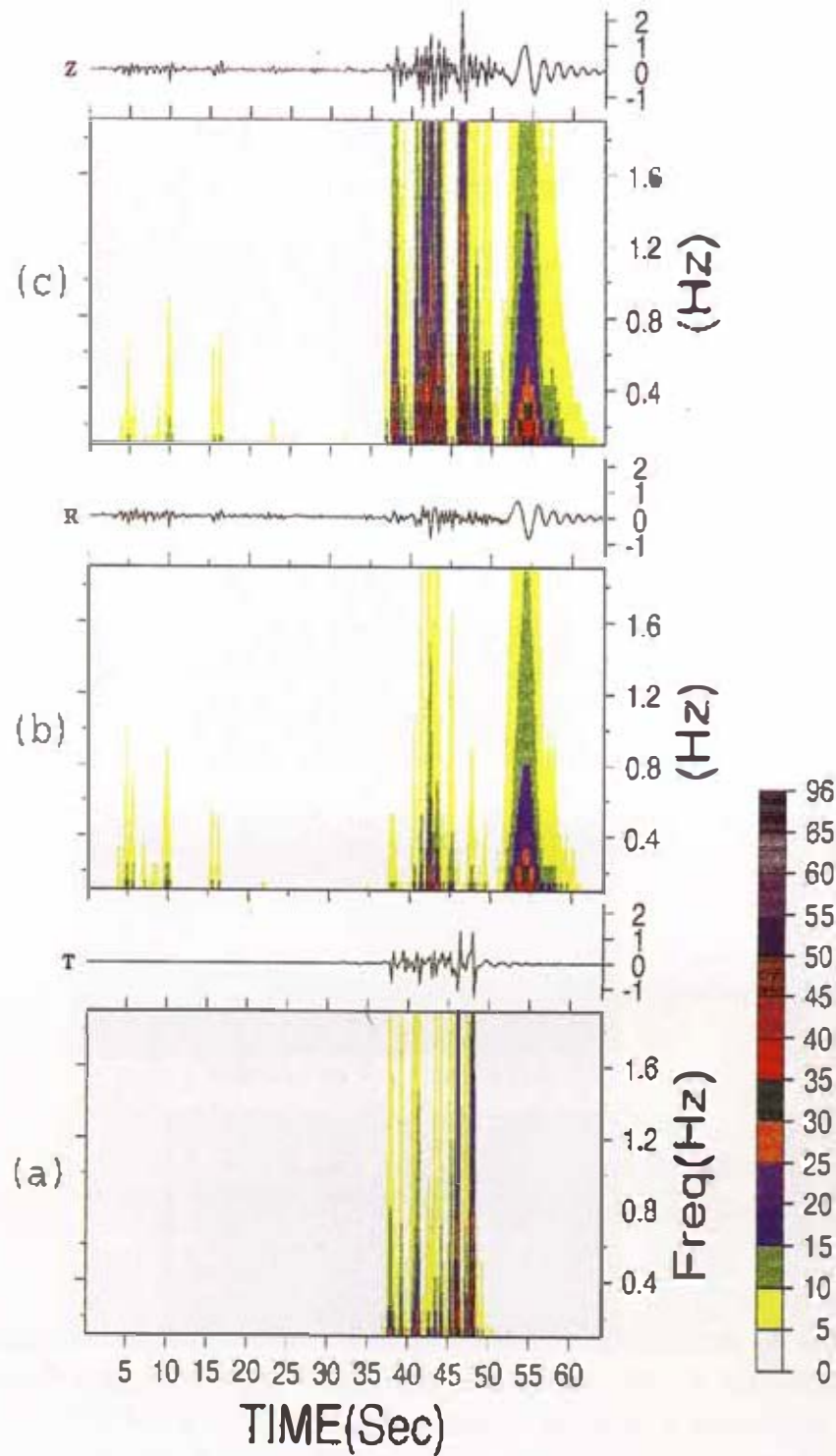


Fig. 1. 3-component synthetic seismograms and corresponding time-frequency representation of (a) the tangential (b) the radial and (c) the vertical component, respectively. Local structure in TF plane is captured after wavelet transform (see text).

The coherency matrix can be written as

$$C = \begin{pmatrix} \langle a_z^2 \rangle & \langle a_z a_x e^{j\psi} \rangle & \langle a_z a_y e^{j\psi} \rangle \\ \langle a_x a_z e^{-j\psi} \rangle & \langle a_x^2 \rangle & \langle a_x a_y \rangle \\ \langle a_y a_z e^{-j\psi} \rangle & \langle a_x a_y \rangle & \langle a_y^2 \rangle \end{pmatrix} \quad (5)$$

where z , x and y are taken to represent the vertical, east-west and north-south directions, respectively. The symbol ψ stands for the phase difference between the vertical and the horizontal components. There are three eigenvalues, namely λ_1 , λ_2 and λ_3 , for the eigensolution of C matrix. For the complete polarization (without noise), only one eigenvalue exist, and the corresponding eigenvector is in the form

$$U = \begin{pmatrix} z_r \\ x_r + jx_i \\ y_r + jy_i \end{pmatrix} = \begin{pmatrix} \bar{a}_z \\ \bar{a}_x \cos \psi - j\bar{a}_x \sin \psi \\ \bar{a}_y \sin \psi - j\bar{a}_y \sin \psi \end{pmatrix} = \begin{pmatrix} \bar{a}_z \\ \bar{a}_h \cos \theta \cos \psi - j\bar{a}_h \cos \theta \sin \psi \\ \bar{a}_h \sin \theta \cos \psi - j\bar{a}_h \sin \theta \sin \psi \end{pmatrix} \quad (6)$$

where \bar{a}_h is the horizontal projection.

The phase difference ψ between the vertical and horizontal components is

$$\psi = \arctan\left(\frac{-x_i}{x_r}\right) = \arctan\left(\frac{-y_i}{y_r}\right), \quad (7)$$

and the strike (θ) of polarization is given by

$$\theta = \arctan\left(\frac{y_r}{x_r}\right) = \arctan\left(\frac{y_i}{x_i}\right), \quad (8)$$

The strength of polarization, p , is

$$p = 1 - \frac{\lambda_2 + \lambda_3}{\lambda_1} \quad (9)$$

where λ_1 , λ_2 and λ_3 are the eigenvalues of the C matrix in descending order. Another parameter is the rectilinearity, e , which is calculated from Vidale's method (Vidale, 1986).

The above polarization analysis is performed through each $CWT_f(a, b)$ of the 3-component seismograms, and each parameter ψ , θ , p and e is then displayed in the time-frequency domain. We start with the same synthetic seismograms as in Figure 1. $CWT_f(a, b)$ results in Figure 1 that have a great frequency component are used for polarization analysis, and the processed results are illustrated in Figure 2-(a), 2-(b), 2-(c) and 2-(d) for the parameters ψ , θ , p and e , respectively.

The phase difference for the pure P-wave is 0° and for the pure S-wave it is $\pm 180^\circ$. The others lie between 0° and 180° (Shieh, 1996). Figure 2-(a) shows two phenomena. (1) Most of

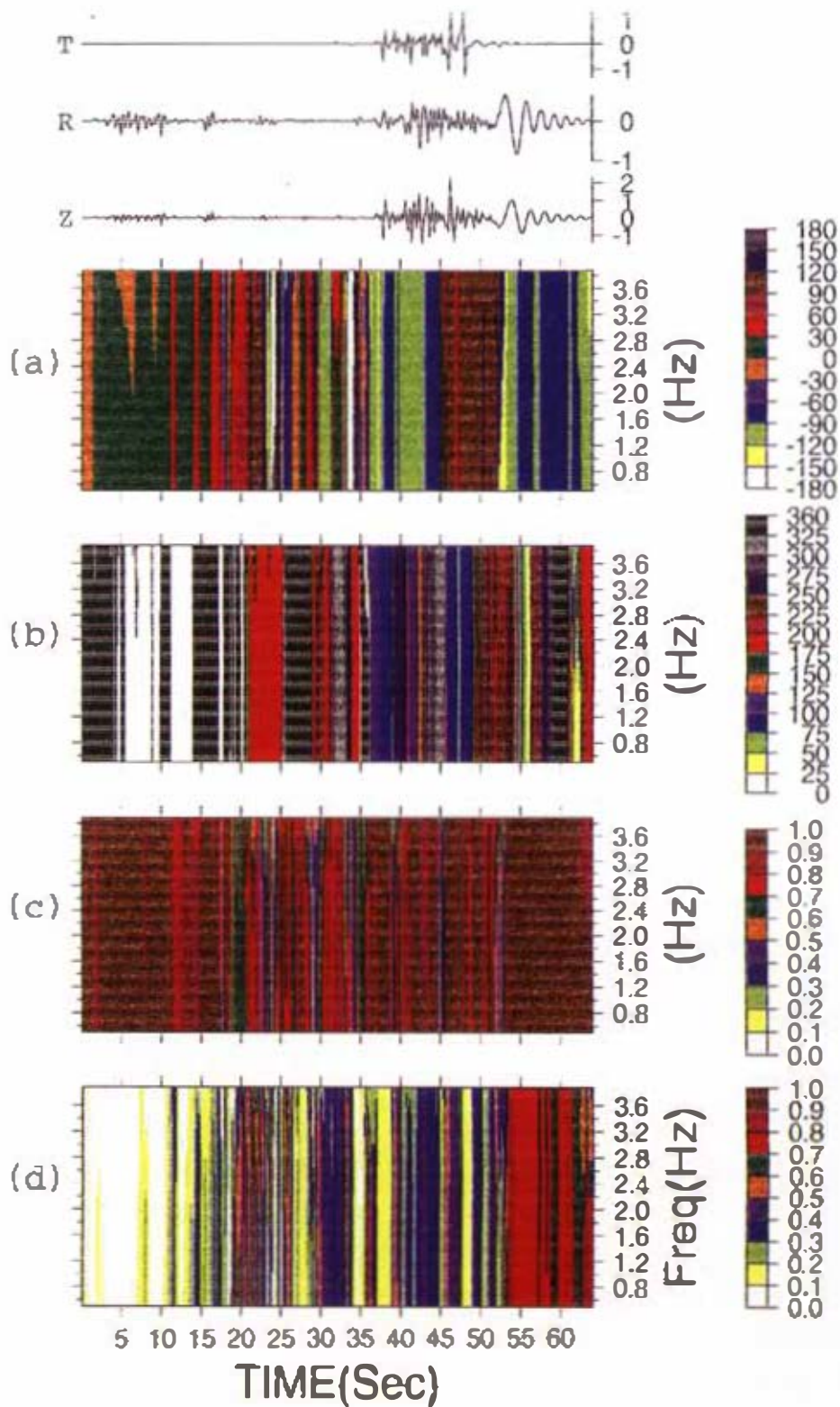


Fig. 2. Results of wavelet-based polarization analysis with the parameters of (a) the phase difference between the vertical and the horizontal components (b) the strike of polarization (c) the strength of polarization (d) the ellipticity.

the body waves have a phase difference near 0° , which indicates that most of them are P-waves. The non-linear motion of some of the body waves is due to the superimposition. (2) The phase difference of the surface waves lie between 30° and 120° . The strike is the direction of the particle motion in the horizontal plane, as measured from the radial direction in this synthetic case. For the linear P-, SV-waves and nonlinear Raleigh waves, the strike is 0° or 180° ; for the Love waves, the strike is 90° or 270° . In Figure 2-(b), it is obvious that most of the strikes are near either 0° or 180° , except for the higher mode surface waves where Love waves are the dominant signal. The strength of polarization (p) contains the information on the S/N ratio. For pure signals, $p=1.0$, unless the signals are mixed together. Clearly, the p values are very close to 1.0 for most of Figure 2-(c). The small number of exceptions (small p) are due to superimposing. The ellipticity (e) is used to evaluate the shape of the motion of particle. In Figure 2-(d), most of the body waves are linear so that their ellipticity is near 0; for the portion of the superimposition, the value of e varies rapidly. It is interesting to note that the value of e varies considerably and lies between 0.3 and 0.6 for the higher mode surface waves, while it varies little and lies between 0.6 and 0.8 for the fundamental mode surface waves. This is not surprising since while the higher mode surface wave behavior is much closer to linear motion, the fundamental mode wave behavior much closer to circular motion.

It may be doubted that conventional polarization analysis provides similar results as for this synthetic case. However, the characteristics shown in Figure 2 that depend slightly on frequency are only available by time-frequency analysis. The differences could be significant for real data (see Jonathan and Park, 1995) when signals with different frequency components are superimposed at the same time interval. In the most probable situation for the observed data, one can separate the data only by both time and frequency decompositions, which is the advantage provided by using the wavelet transform.

5. DISCUSSION

Wavelet transform is a new mathematical tool that is used to get more information from the study of the local structure of the signal in the time-frequency domain. Many scientists predict that it may play an important role in the next decade, though there are several unsolved problems. However, wavelet theory is in its initial stages and further investigation on the theoretical approach and application is needed. Since wavelet-based seismogram analysis is not well discussed in the literature, this article first introduces the fundamental concept of wavelet transform, and then constructs a direct bridge between the feature of polarization analysis in the time-frequency and seismogram analysis. The processed results (Figure 1 and 2) show many interesting features that provide more useful information than was available before. Furthermore, its applicability to real, complicated seismograms can be expected.

Acknowledgements The authors would like to thank Dr. Gwo-Bin Ou for providing the synthetic seismograms. Several constructive and friendly comments suggested by two anonymous reviewers are highly appreciate. In addition, the authors thank the editor for the time he spent.

REFERENCES

- Allen, J. B., and L. R. Rabiner 1977: A unified approach to short-time Fourier analysis and synthesis. *Proc. IEEE*, **65**, 1558-1564.
- Beylkin, G., R. Coifman, and Rokhlin, R. 1991: Fast wavelet transforms and numerical algorithms, I. *Comm. Pure Appl. Math*, **44**, 141-183.
- Cohen, A., 1989: Time-frequency distributions: A review. *Proc. IEEE*, **77**, 941-981.
- Coifman, R. R., and M. V. Wickerhauser, 1992: Wavelet analysis and signal processing. in *Wavelets and Their Applications*. In: M. B. Ruskai et al. (Eds.), Jones and Bartlett, Boston, 153-178.
- Daubechies, I., 1988: Orthonormal bases of compactly supported wavelets. *Commun. Pure Appl. Math.*, **1**, 909-996.
- Daubechies, I., 1992: *Ten Lectures on Wavelets*. SIAM, Philadelphia.
- Gabor, D., 1946: Theory of communication, *Journ. IEEE*, **93**, 429-457.
- Goupillaud, P., A. Grossmann, and J. Morlet, 1984: Cycle-octave and related transforms in seismic signal analysis. *Geoplotation*, **23**, 85-102.
- Grossmann, A., and J. Morlet, 1984: Decomposition of Hardy function into square integrable wavelets of constant shape. *SIAM J. Math. Anal.*, **15**, 723-736.
- Grossmann, A., R. Kronland-Martinet, and J. Morlet, 1989: Reading and understanding wavelet transforms. *WAV*, **89**, 2-20.
- Jonathan, B. D., and D. L. Donoho, 1995: WaveLab and reproducible research, *Wavelets and Statistics, Lecture Note in statistics*. In: A. Antoniadis and G. Oppenheim, Springer-Verlag, 55-81.
- Jones, D. L., and R. G. Baraniuk, 1991: Efficient approximation of continuous wavelet transforms. *Electronic lett*, **27**, 748-750.
- Jonathan M. L., and J. Park, 1995: Multiwavelet spectral and polarization analysis of seismic records. *Geophys. J. Int.*, **122**, 1001-1021.
- Lamari, P. G., and Y. Meyer, 1986: Ondelettes et bases hilbertiennes. *Rev. Math. Iberoamericana*, **2**, 1-18.
- Mallat, S., 1989: A theory for multiresolution signal decomposition: The wavelet representation, *IEEE Trans. Patt. Anal. Machine Intell*, **11**, 674-693.
- Mallat, S., and Z. Zhang, 1993: Matching pursuit with time frequency dictionaries. *IEEE Trans. signal prec.*, **41**, 3397-3415.
- Meyer, Y., 1990: *Ondelettes et Operateurs*, **3**, Paris: Herman.
- Meyer, Y., 1993: *Wavelets: Algorithms and Applications*. SIAM: Philadelphia.
- Press, W. H., S. A. Teukolsky, W. T. Vetterling, and B. P. Flannery, 1992: *Numerical Recipes in FORTRAN*, 2nd edn, Cambridge University Press, Cambridge.
- Rabiner, L. R., R. W. Schafer, and C. M. Rader, 1969: The chirp Z-transform algorithm, *IEEE Trans*, **AU-17(2)**, 86-92.
- Rioul, O., and M. Vetterli, 1991: Wavelets and signal processing. *IEEE, Trans. Signal Proc. Mag.*, 14-38.

- Shieh, C. F., 1996: Polarized correlation between 3-component seismograms. *Physics of the Earth and Planetary interior*, **97**, 197-204.
- Shieh, C. F., and R. B. Herrmann, 1990: Ground roll: Rejection using polarization filters. *Geophysics*, **55**, 1216-1222.
- Vidale, J. H., 1986: Complex polarization analysis of particle motion. *Bull. Seis. Soc. Am.*, **76**, 1393-1405.

AUTHOR INDEX

519

(TAO, VOL. 8, 1997)

Arya, B. C.	371	Lal, M.	247
Bose, S.	247	Lamb, Peter J.	481
Bosilovich, Michael G.	271	Lee, L. C.	345
Cai, H. J.	345	Lee, Mon-Feng	13
Chang, Yet-Chung	461	Li, Yuan-Hui	405
Chau, Ha Duyen	155	Liang, Wen-Tzong	329
Chen, Chen-Tung A.	405	Lin, Cheng-Horng	329
Chen, Chia-Rong	481	Lin, Ching-Ren	329
Chen, Chien-Chih	443	Lin, Hsin-Mu	385
Chen, Chow-Son	443	Lin, K. H.	165
Chen, Kou-Cheng	329	Liu, Gin-Rong	95
Chen, Min-Te	111	Liu, J. Y.	165, 221
Chen, George Tai-Jen	427	Liu, Tsung-Kweiliu	313
Chen, Jung-Nan	255	Lu, Cheng-Fu	427
Chen, Kuei-Pao	295	Ma, Chung-Ping	461
Chen, Sen-Wen	213	Ma, Kuo-Fong	13
Chen, Wann-Jin	95	Ma, S. Y.	179
Cheng, Kang	213	Maitra, A.	247
Cheng, Ping-Hu	313	Meehan, Dan	189
Cheng, Shih-Nan	31	Min, Wei	69
Chern, Jiun-Dar	271	Nam, Vu Hong	155
Chiu, Jer-Ming	329	Niranjana, K.	239
Chung, Yu-Chia	141, 255	Prasad, D S V V D	203
Ghosh, A. B.	247	Prell, Warren L.	111
Hao, Truong Quang	155	Ram, P Sri	203
Hou, Tsai-Yuan	329	Rao, P V S Rama	203
Huang, Bor-Shouh	1, 329	Reddy, Y. Sreenivasa	239
Huang, C. R.	165	Schmidt, B. R.	345
Huang, Yinn-Nien	213	Shen, Yng-Yuan	313
Hung, Jia-Jang	405	Shieh, Chiou-Fen	509
Huang, Zerong	233	Shih, Ruey-Chyuan	1
Huh, Chih-An	289	Singh, S. K.	371
Igarashi, Kiyoshi	165	Son, Vo Thanh	155
Jain, S. L.	371	Song, Gwo-Shyh	461
Jamid, A.	371	Sun, Wen-Yih	271
Jayachandran, P T	203	Sung, Quocheng	313
Kung, Ernest C.	69	Thoa, Nguyen Thi Kim	155

AUTHOR INDEX

(TAO, VOL. 8, 1997)

Thulasiraman, S.	239	Wu, Hsin-Hung	355
Tri, Pham Van	155	Wu, Q.	179
Tripathi, O. P.	371	Xu, Chufu	165
Truong, Luong Van	155	Xu, J. S.	179, 165
Tsai, Chu-Chuan Peter	49	Yang, Chieh-Hou	313
Tsai, Lung-Chih	221	Yen, Horng-Yuan	329
Tsai, W. H.	165	Yeh, Jeh-Chyi	141
Tsai, Yi-Ben	355	Yeh, Yih-Hsiung	329
Wang, Chien-Ying	295	Yen, K. C.	165
Wang, Jim	509	Yu, D. C.	165
Wang, Pao K.	385	Yu, Ting-To	31
Wang, W. X.	165	Zeng, Wen	233
Whang, Y. C.	345	Zhang, Xunjie	233

VOLUME CONTENTS

521

(TAO, VOL. 8, 1997)

Vol. 8, No. 1

ARTICLES

Numerical Modeling for Elastic Wave Propagation With a Hybrid of the Pseudo-Spectrum and Finite-Element Methods.....	
.....Bor-Shouh Huang and Ruey-Chyuan Shih	1
Simulation of Historical Tsunamis in the Taiwan Region	
.....Kuo-Fong Ma and Mon-Feng Lee	13
Relationships of Seismic Source Scaling in the Taiwan Region.....	
.....Chu-Chuan Peter Tsai	31
Stress Diffusion and Spatial Migration of Aftershocks in the Hualien Area, Taiwan.....	
.....Ting-To Yu and Shih-Nan Cheng	51
A Spectral Analysis of Wave Activities and Blocking in the Northern Hemisphere Winter.....	
.....Wei Min and Ernest C. Kung	69
Systematic Error Correction of GMS-4 IR Data.....	
.....Gin-Rong Liu and Wann-Jin Chen	95
Reassessment of CLIMAP Methods for Estimating Quaternary Sea-Surface Temperatures: Examination Using Pacific Coretop Data Sets.....	
..... Min-Te Chen and Warren L. Prell	111
^{228}Ra and ^{226}Ra Distributions off North and Southwest Taiwan.....	
.....Jeh-Chyi Yeh and Yu-Chia Chung	141

Vol. 8, No. 2

ARTICLES

Magnetic and Ionospheric Observations During the October 24, 1995 Total Solar Eclipse in Vietnam.	
.....Nguyen Thi Kim Thoa, Ha Duyen Chau, Truong Quang Hao, Pham Van Tri, Vo Thanh Son, Luong Van Truong and Vu Hong Nam	155
Ionospheric Response to a Solar Eclipse in the Equatorial Anomaly Region	
..... K. C. Yeh, D. C. Yu, K. H. Liu, C. R. Huang, W. H. Tsai, J. Y. Liu, J. S. Xu, Kiyoshi Igarashi, Chufu Xu and W. X. Wang	165

VOLUME CONTENTS

(TAO, VOL. 8, 1997)

Observations of the Ionospheric Total Electron Contents During the Solar Eclipse of October 24, 1995 by using the GPS Beacon.....J. S. Xu, S. Y. Ma and Q. Wu	179
HF Doppler Backscatter Observations of the October 1995 Total Solar Eclipse.....Dan Meehan	189
Ionospheric Changes Observed Over Waltair (Dip 20N) During the Total solar Eclipse of 24th October 1995.....P V S Rama Rao, D S V V D Prasad, P Sri Ram and P T Jayachandran	203
Traveling Ionospheric Disturbances Detected During the Solar Eclipse of 24 October 1995.....Kang Cheng, Yinn-Nien Huang and Sen-Wen Chen	213
Ionospheric Observations of the Solar Eclipse on Oct. 24, 1995 at Chung-Li.....Lung-Chih Tsai and Jann-Yenq Liu	221
Ionospheric Absorption Effects of the Solar Eclipse of 24 October 1995.....Zeng Wen, Zhang Xunjie and Huang Zerong	233
Indications of Atmospheric Ozone Decrease in Solar UV-B Flux Changes During the Total Solar Eclipse of 24 October 1995.....K. Niranjan, S. Thulasiraman and Y. Sreenivasa Redd	239
Ground-based Measurements of Some Minor Constituents During the Solar Eclipse - 1995.....A. B. Ghosh, S. Bose, M. Lal and A. Maitra	247

Vol. 8, No. 3**ARTICLES**

²²⁶ Ra, ²¹⁰ Pb and ²¹⁰ Po Distributions at the Sea off Southern Taiwan: Radioactive Disequilibria and Temporal Variations.....Jung-Nan Chen and Yu-Chia Chung	255
Regional Response of the NCAR CCM1 to Anomalous Surface Properties.....Wen-Yih Sun, Michael G. Bosilovich and Jiun-Dar Chern	271
²⁴⁰ Pu/ ²³⁹ Pu Ratios in Sun Moon Lake Sediments: Implications for Sources of Nuclear Fallout in Taiwan.....Chih-An Huh	289

VOLUME CONTENTS

523

(TAO, VOL. 8, 1997)

A Seismic Refraction Profile Across the Longitudinal Valley Near Hualien, Taiwan.....	Chien-Ying Wang and Kuei-Pao Chen	295
Mapping of Groundwater With the Direct Current Resistivity Method in the Area Between the Pachang-Chi and Tsengwen-Chi, Southern Taiwan.....Chieh-Hou Yang, Ping-Hu Cheng, Yng-Yuan Shen, Tsung-Kweiliu Liu, Quocheng Sung	313
A High-Resolution Seismic Array Experiment in the Hualien Area, Taiwan	Yih-Hsiung Yeh, Horng-Yuan Yen, Kou-Cheng Chen, Jer-Ming Chiu, Cheng-Horng Lin, Wen-Tzong Liang, Bor-Shouh Huang, Ching-Ren Lin and Tsai-Yuan Hou	329
A Simulation Study of the Interaction Between a Fast Shock and the Heliopause.....	L. C. Lee, B. R. Schmidt, H. J. Cai and Y. C. Whang	345

NOTE AND CORRESPONDENCE

A Study of the Errors in Locating Earthquakes due to the Geometry of the Taiwan Seismic Network.....	Yi-Ben Tsai and Hsin-Hung Wu	355
--	------------------------------	-----

Vol. 8, No. 4

ARTICLES

Measurement of Various Atmospheric Parameters During a Total Solar Eclipse.....	S. L. Jain, B. C. Arya, S. K. Singh, O. P. Tripathi and A. Hamid	371
A Numerical Study of Microphysical Processes in the 21 June 1991 Northern Taiwan Mesoscale Precipitation System.....	Hsin-Mu Lin and Pao K. Wang	385
Aquatic Chemistry of Lakes and Reservoirs in Taiwan.....Yuan-Hui Li, Chen-Tung A. Chen and Jia-Jang Hung	405
On the Climatological Aspects of Explosive Cyclones Over the Western North Pacific and East Asia Coastal Areas.....	George Tai-Jen Chen and Cheng-Fu Lu	427
Geoelectrical Surveys of Southwestern Taiwan.....Chow-Son Chen and Chien-Chih Chen	443

VOLUME CONTENTS

(TAO, VOL. 8, 1997)

Characteristics of Submarine Topography off Northern Taiwan.....Gwo-Shyh Song, Yet-Chung Chang and Chung-Ping Ma	461
Improved Treatment of Surface Evapotranspiration in a Mesoscale Numerical Model Part I: Via the Installation of the Penman-Monteith Method.....Chia-Rong Chen and Peter J. Lamb	481

NOTE AND CORRESPONDENCE

Wavelet Transform and 3-Component Seismogram Analysis.....Chiou-Fen Shieh and Jim Wang	509
---	-----